

Measuring high-slope parts using coherence scanning interferometry

Martin F. Fay, Xavier Colonna de Lega, and Michael Schmidt
Zygo Corporation
Middlefield, CT

INTRODUCTION

Measuring high-slope machined parts often forces an unsatisfying compromise between sufficient data coverage and acceptable throughput, as metrology tools generally entail some sort of tradeoff between slope acceptance and measurement speed. For example, for optical systems higher-NA objectives have higher slope acceptance but generally smaller fields of view (FOV), meaning more individual measurements if the region of interest exceeds a single FOV.

Recessed and large-departure features pose the additional challenge of imposing a minimum working distance, which also generally entails a tradeoff with slope acceptance.

Coherence scanning interferometry (CSI) is commonly used to measure machined parts, providing non-contact areal topography maps with typical single-measurement topography repeatability of less than a nm on smooth, high-reflectivity surfaces [1]-[2]. Typical selection of objective magnification ranges from about 1X to about 100X.

Ideally the highest local slope θ_{max} is accommodated within the specular limit of the objective NA, satisfying $NA > \sin(\theta_{max})$. In practice a lower-NA objective may be prescribed by constraints on minimum working distance or field-size/throughput; or by practical considerations such as cost and availability. Fortunately, measuring slopes beyond the specular limit is possible provided some light is scattered (generally by surface roughness) and the measurement is sufficiently sensitive. Even so, in the past CSI has often been challenged by high-slope parts.

Recent advances in the technology both significantly improve the baseline sensitivity of CSI and enable high-dynamic-range operation, allowing measurement of recessed or high-slope features that were previously inaccessible, or over larger fields of view for improved throughput.

MEASUREMENT & ANALYSIS

A variety of machined parts were measured using a modern commercial CSI microscope [3]. As shown schematically in FIGURE 1, CSI operates by scanning an interferometric objective relative to the sample being measured, producing localized interference patterns which define sample height at each pixel of the camera. Thus a single scan produces areal topography data at corresponding positions of best focus over the full field of the camera. Any type of interferometric objective can be used, including Mirau, Michelson, Linnik, or wide-field [4]-[5] objectives.

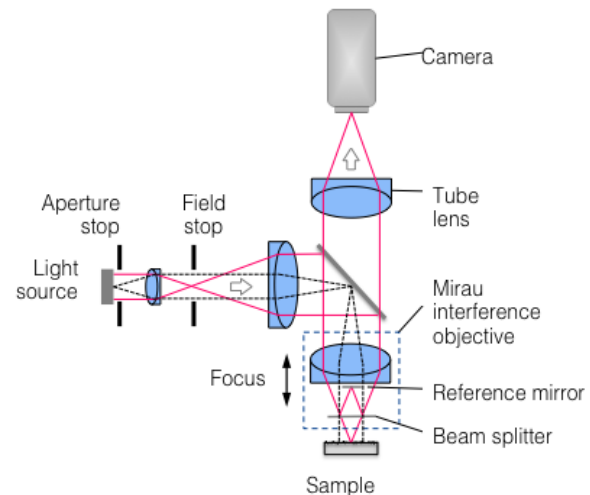


FIGURE 1. Schematic representation of Coherence Scanning Interferometry.

For the results presented here, the baseline data acquisition time is about 0.14 seconds per micron scanned. All surface plots shown represent raw height data without smoothing, masking or interpolation of missing data points. Particularly weak signals were detected using dynamic noise reduction (DNR), which allows a user-specified trade-off between throughput and sensitivity while preserving full vertical and lateral resolution [6].

SLOPES BEYOND THE SPECULAR LIMIT

FIGURE 2 shows a diamond-turned cone with an included angle of 90° , an outermost diameter of 4 mm, and relatively low surface roughness ($S_a \sim 1.1$ nm, as measured at normal incidence with a 10X Michelson objective). Accommodating the 45° slopes within the specular limit requires an objective with $NA > 0.7$, but in practice this would entail stitching over hundreds of FOV, likely with unacceptable throughput.

At the other extreme, measuring the cone within a single FOV requires a low-mag objective with NA well below 0.7. Attempting such a measurement with conventional CSI might yield only sparse data along the cone, but also a valuable hint: data at slopes above the specular limit suggest detectable scattered light.

Using a 2.5X Michelson objective ($NA = 0.075$) in conjunction with 4X DNR (16X increase in baseline measurement time), near-complete data coverage is achieved. These data are well-suited for measuring cone angle and roundness.

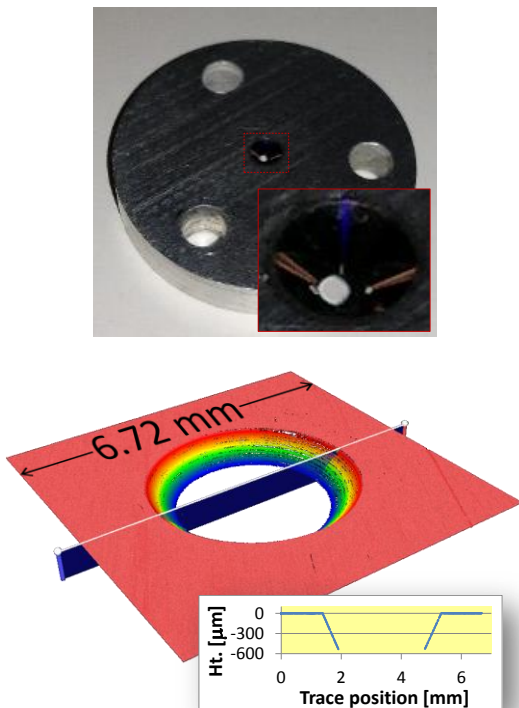


FIGURE 2. Measurement of 5-mm-diameter diamond-turned 90° cone in a single FOV. Top: photograph of part; bottom: measured height map.

Spherical features exhibit slopes approaching 90° and occur in a wide variety of applications, such as ball bearings and sealing surfaces. The challenge of measuring spherical features grows with increasing diameter: high slopes remain alongside requirements for increasing FOV and working distance.

FIGURE 3 shows a 3-mm-diameter fuel-injector sealing ball as measured in a single FOV with a 5.5X Michelson ($NA = 0.15$). Data coverage is near-complete for local slopes beyond 60° . Surface roughness S_a is about $0.1 \mu\text{m}$ as measured with this same objective.

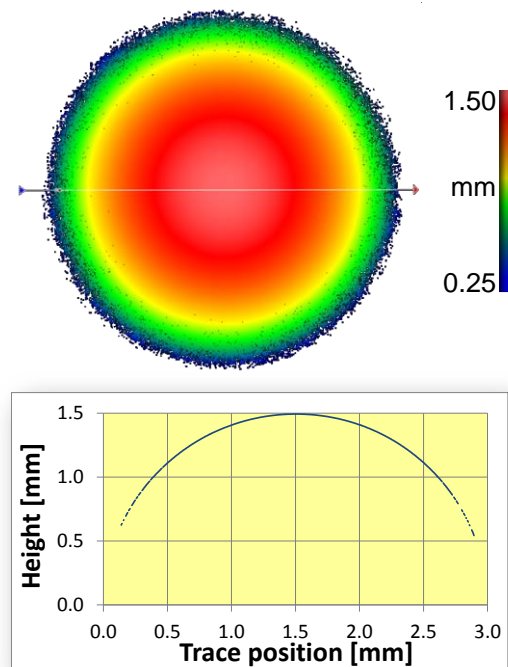


FIGURE 3. 3-mm-diameter sealing ball measured in a single FOV for local slopes up to 60° .

Access to larger FOVs offers advantages even when stitching is still required. Improved throughput is an obvious benefit, but larger FOVs also enable faster targeting of functional surfaces and registration to datum surfaces. Using fewer FOVs also reduces form error that can arise from stitching multiple slivers of data from smaller-aperture height maps.

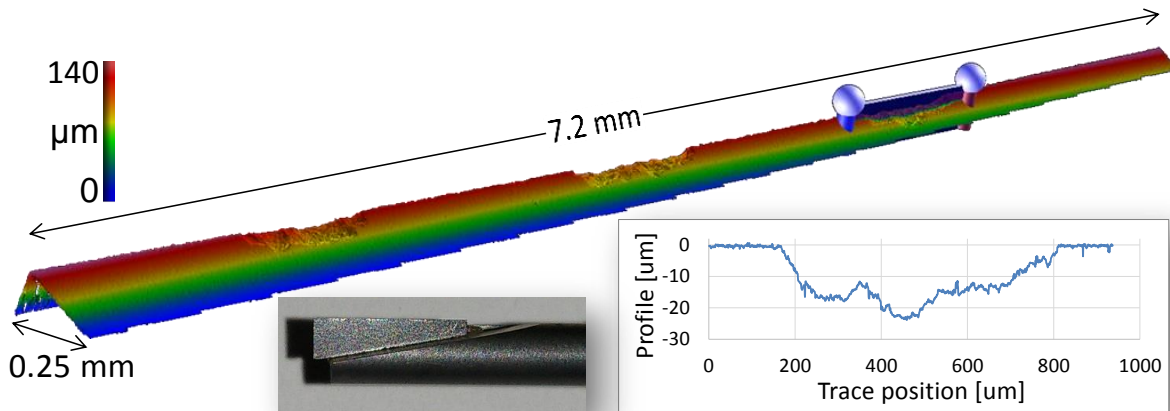


FIGURE 4. End-mill measured with $0.4\ \mu\text{m}$ lateral sampling over 7.2-mm length and $145\text{-}\mu\text{m}$ scan range in about 9 minutes. Photograph of part is shown in lower left inset.

FIGURE 4 shows a diamond end-mill [7] that was subjected to wear experiments in three locations, producing local slopes exceeding 70° . On the face of it this might appear to call for stitching hundreds of high-NA measurements. However, full data coverage was achieved by stitching only ~ 20 FOVs using a 20X Mirau objective ($\text{NA} = 0.4$, specular limit $\sim 23^\circ$), yielding $0.4\text{-}\mu\text{m}$ lateral sampling ($0.9\text{-}\mu\text{m}$ optical resolution) and nm-scale vertical resolution over the entire tool length with a total measurement time of only 9 minutes.

Note that success in measuring slopes beyond the specular limit depends on multiple contributions, including the S_a of the sample and spatial-frequency-dependent variations of the surface roughness.

RECESSED HIGH SLOPES

Sometimes high-slope features are recessed, residing some distance below a neighboring feature. Common examples include cones inside bores and shoulders along the outside of a shaft. Recessed features can play functional roles, for example as mounting or sealing surfaces, with corresponding critical parameters such radius, roundness and angle.

Optically measuring these critical parameters requires an objective with sufficient working distance to accommodate the depth of recession. This effectively limits options to lower-NA objectives, meaning measurements must make use of whatever scattered light there might be. With conventional CSI, measuring some extreme cases of recessed high slopes might previously have been impractical.

FIGURE 5 shows a photograph of an unfinished fuel injector with surface roughness $S_a \sim 1\ \mu\text{m}$. The highlighted region indicates a shoulder where the fuel injector mounts against an engine block. The geometry of this shoulder is critical for proper sealing and can be characterized by the circumferential radius formed at the intersection of two steep-slope regions.

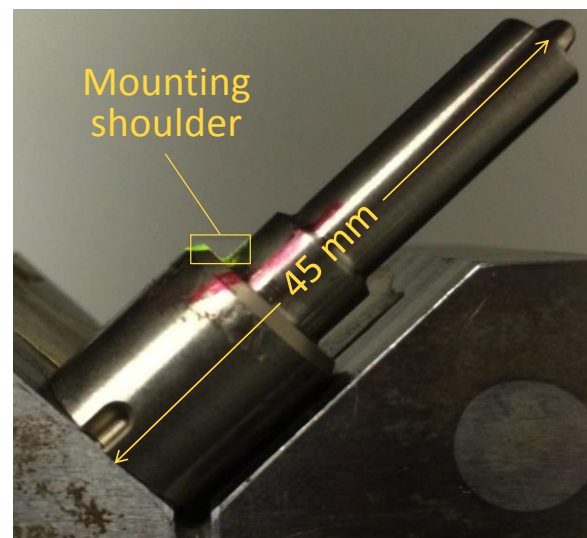


FIGURE 5. Photograph of fuel injector, with mounting shoulder region outlined in yellow.

Measuring the shoulder region previously required stitching multiple higher-magnification measurements, along with great care to avoid mechanical interference with the rest of the part. FIGURE 6 shows a measurement captured in a single FOV of a specialized 5X Michelson ($\text{NA} = 0.12$) with a working distance of 40 mm.

Near-complete data coverage is achieved in spite of local slopes up to 45° .

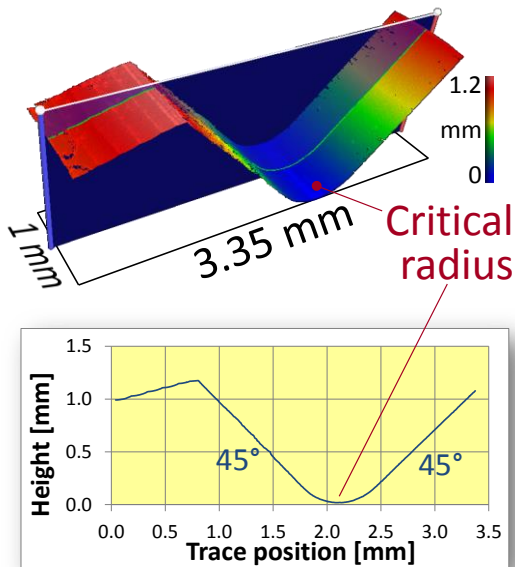


FIGURE 6. Measurement of shoulder region of fuel injector, highlighting radius critical for proper sealing with engine block.

FIGURE 7 shows an electrical feed-through assembly comprising an array of ~ 1 -cm pins secured by glass cladding which is recessed by ~ 1 mm within a metal housing. In addition to the obstructing pins, challenges with measuring the glass profile include moderate local slope up to $\sim 15^\circ$ and comparatively weak scattering due to low roughness and refractive index.

Results obtained using a 5.5X Michelson ($NA = 0.15$) show near-complete data coverage of the glass cladding, with missing points corresponding primarily to the location of the encased pins. To efficiently accommodate the wide range of part reflectance (metal vs. tilted glass), a high dynamic range (HDR) mode was used combining scans at varying light levels [6].

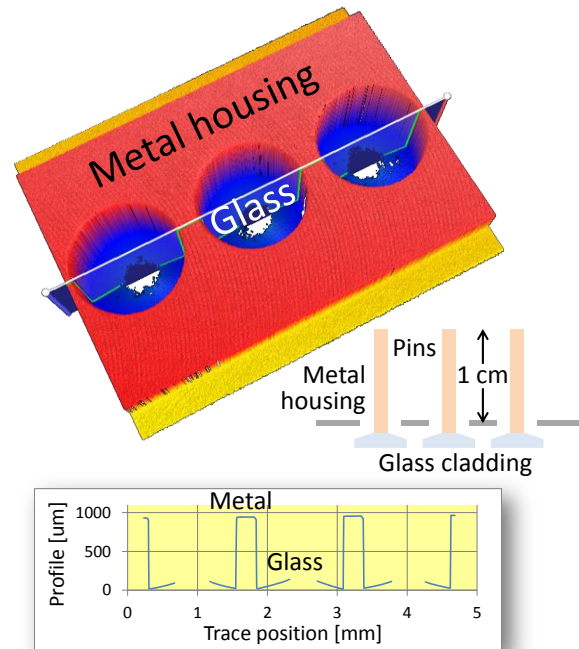


FIGURE 7. Electrical feed-through assembly. Of primary interest is the glass cladding, recessed below the metal housing along with pins extending ~ 1 cm beyond the housing. Blue regions in the height map correspond to glass, with missing data indicating the location of pins.

NEAR-VERTICAL SLOPES

Maximum measurable slope is a function of objective NA along with the effective reflectivity of the surface being measured. The examples shown so far have predominantly showcased measurements using lower NA objectives. How high can measured slopes become at higher NA?

FIGURE 8 shows that for a hypodermic needle measured *end-on* in a single FOV using a 50X Mirau objective ($NA = 0.55$, specular limit $\sim 33^\circ$), the answer is *arbitrarily close to vertical*. Data are obtained on all beveled surfaces with prevailing slopes of 74° and 82° , and also along the near-vertical outer tube surface where the slope exceeds 89° . Again, no interpolation is performed, nor is there any masking: the bore region is free of false data.

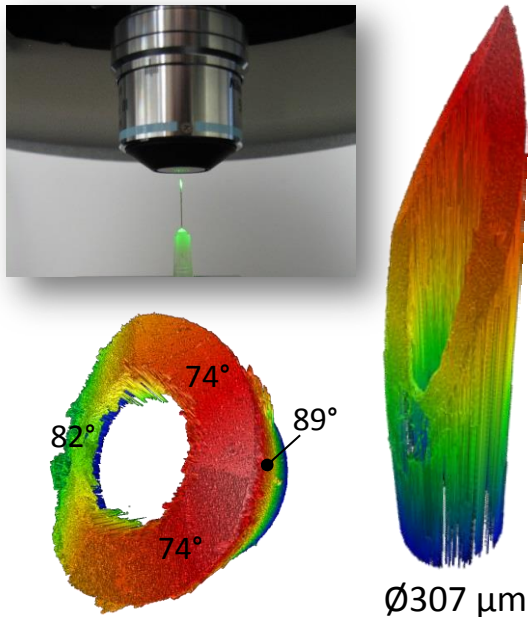


FIGURE 8. Hypodermic needle measured end-on in a single FOV. Upper left: photograph of setup. Right: obtained data over 1.8-mm scan range. Lower left: same data rotated to show measured slopes up to 89° and automatic identification of bore region.

CONCLUSION

With recent advances that improve sensitivity to weak interferometric signals, CSI can now measure recessed and high-slope features that previously may have been considered beyond the reach of the technology. In addition to improving baseline sensitivity, these advances include tools to further extend dynamic range such as DNR and HDR [6]. As seen in the examples, measured slopes as high as 89° have now been demonstrated.

More generally, the improvements enable wider latitude in objective selection, allowing operation over larger fields of view for increased throughput and at greater working distances for improved ease of use.

ACKNOWLEDGMENTS

The original work presented in this paper benefited from key contributions and input from Eric Felkel, Nate Gilfoy, Mackenzie Massey, and Dan Russano.

REFERENCES

- [1] de Groot P. Coherence Scanning Interferometry. In: Leach R, editor. Optical

- Measurement of Surface Topography. Berlin: Springer Verlag; 2011. p. 187-208.
- [2] ISO, [25178-604:2013(E): Geometrical product specification (GPS) – Surface texture: Areal – Nominal characteristics of non-contact (coherence scanning interferometric microscopy) instruments] International Organization for Standardization, Geneva (2013).
- [3] Zygo Corporation, [NexView Optical Profiler], Specification sheet SS-0095 09/12 (2013).
- [4] J. Biegen, X. Colonna de Lega and P. de Groot, "Wide-field interference microscopy for areal topography of precision engineered surface," Proc. ASPE annual meeting, paper 4111 (Boston, 2014).
- [5] P. J. de Groot, L. L. Deck, J. F. Biegen and C. Koliopoulos "Equal-path interferometer", US Patent 8,045,175 (2011).
- [6] Fay, M. F., Colonna de Lega, X., and de Groot, P. Measuring high-slope and super-smooth optics with high-dynamic-range coherence scanning interferometry. Proc. OSA, 2014: Paper 1981102.
- [7] Thanks to Professor Chris Evans and Chris Tyler at the University of North Carolina at Charlotte (Mechanical Engineering and Engineering Science).